William G. Bradley, Jr., M.D., Ph.D.
Victor Waluch, M.D., Ph.D.[2]

Blood Flow: Magnetic Resonance Imaging[1]

The appearance of flowing fluid has been evaluated in several clinical situations using a flow phantom, computer simulation, and clinical magnetic resonance (MR) images. Unsaturated protons just entering the imaging volume can emit a strong signal relative to the partially saturated adjacent tissue ("flow-related enhancement"). Slow laminar flow in veins can be distinguished on the basis of a stronger second echo due to rephasing effects ("even echo rephasing"). Synchronization of the cardiac cycle and the MR pulsing sequence produces increased signal in sections acquired during diastole ("diastolic pseudogating"). Intraluminal signal is shown to decrease as velocity is increased ("high velocity signal loss"). Onset of turbulence causes further loss of signal. Direction of flow oblique to the imaging plane can be predicted on the basis of decreased upstream and increased downstream signal.

Index terms: Blood, flow dynamics • Magnetic resonance, experimental

Radiology 1985; 154: 443-450

FLOWING blood has a variable appearance on magnetic resonance (MR) images depending on the velocity and direction of flow (1-6). Rapidly flowing blood generally appears dark. This has been explained on the basis of irradiated protons leaving the selected section prior to emitting a spin echo. Slow flow can produce a bright intraluminal signal and is most pronounced when using partial saturation sequences with short TR times. When multisection acquisition is used, the effect is most significant in the section first encountered by the flowing blood (7).

The effect of velocity on MR signal intensity has provided a basis for the noninvasive determination of blood flow velocity (8-11). This application, however, requires specialized pulsing sequences not generally used for routine clinical imaging. The intent of this paper is to describe various flow phenomena that are readily apparent on MR images obtained using routine clinical pulsing sequences. This approach has the advantage of not requiring additional imaging time because it uses information already present in the MR image.

Increased intraluminal signal during slow flow has been previously labeled "paradoxical enhancement" (3, 4). This phenomenon has been evaluated using a flow phantom and computer simulation. It has been found to arise from two separate phenomena that we call "flow related enhancement" and "even echo rephasing" (12). Increased intraluminal signal can also be found during rapid pulsatile flow on certain sections in a multisection acquisition. This occurs when the cardiac cycle and the MR pulsing sequence happen to coincide so that certain sections are acquired during systole while others are acquired during diastole. Although the mean velocity over the cardiac cycle may be high, the lack of flow during diastole results in high intraluminal signal. We call this "diastolic pseudogating" and have evaluated it with a flow phantom.

Flow phantom experiments have also been performed to evaluate rapid blood flow both perpendicular and oblique to the imaging plane. The "high velocity signal loss" is shown to follow a simple algebraic relationship when flow is perpendicular to the plane of imaging. Upstream signal loss also allows the direction of flow to be determined when it is oblique to the imaging plane.

MATERIALS AND METHODS

A simple flow phantom was constructed of 1-cm ID Tygon tubing as shown in Figure 1. The phantom consisted of a single loop of tubing positioned along the axis of the main magnetic field such that flow was perpendicular to the transverse axial plane. The flow phantom was positioned in the center of the magnet, 1 meter from the entry surface. For simplicity, water was used instead of blood. All measurements were taken relative to a stationary tube of water adjacent to the tubes containing flowing water. This allowed a direct comparison of flowing and stationary fluids without the necessity to consider different magnetic relaxation times or the potential effects of plasma skimming during rapid blood flow (13). Since pure water has a longer T1 time than blood, it must remain within the magnetic field a longer period of time to become fully magnetized. The return loop has a course of 3 meters within the bore of the magnet; this assures essentially full magnetization of water even at the highest velocities used. Images from incoming and return limbs

[1] From the NMR Imaging Laboratory, Huntington Medical Research Institutes and the Department of Radiology (W.G.B.), Huntington Memorial Hospital, Pasadena, CA. Presented at the Sixty-ninth Scientific Assembly and Annual Meeting of the Radiological Society of North America, Chicago, IL, Nov. 13-18, 1983. Received April 25, 1984; revision requested May 31, 1984; accepted July 31, 1984; final revision received Sep. 25, 1984.

[2] Diasonics NMR Fellow.

ht

Figure 1

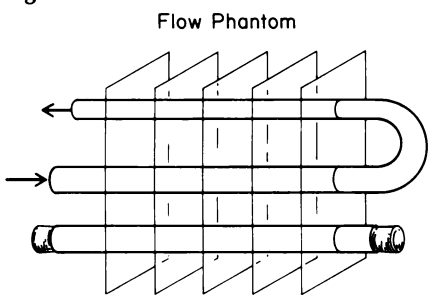

Flow phantom. Loop of 1-cm Tygon tubing is positioned perpendicular to imaging plane. Adjacent tubing with stationary water serves as local reference.

Figure 2

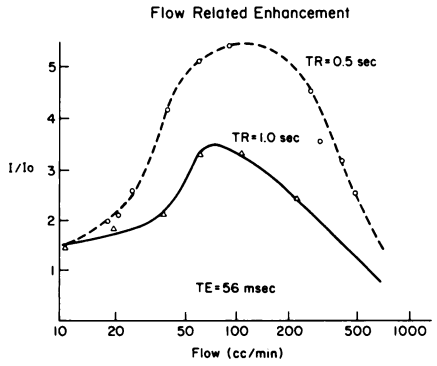

Flow-related enhancement and high-velocity signal loss demonstrated in flow phantom. Intraluminal signal I is initially increased (relative to stationary signal I_0) due to unsaturated protons entering section. Effect is seen at low velocity and is accentuated at short TR. Signal is lost as velocity is increased due to protons leaving section prior to emitting spin echo.

Figure 3

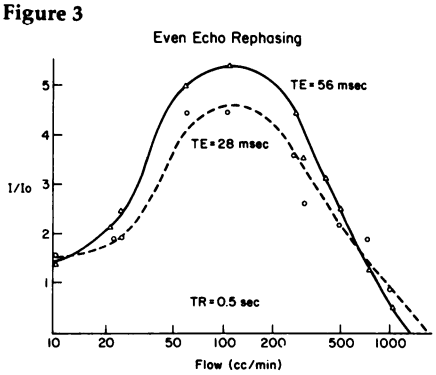

Even-echo rephasing demonstrated in flow phantom. Second echo is more intense than the first in slow laminar flow. This is due to rephasing effects that arise from flow into the section-selecting gradient.

Figure 4

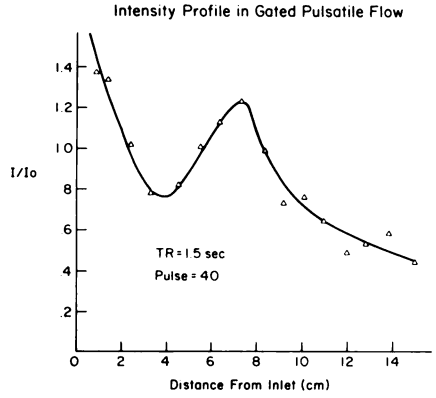

Intensity profile in gated pulsatile flow (flow phantom). Ratio of flowing to stationary water (I/I_0) is plotted as a function of distance from the entry surface during a 15-section acquisition. Increased intensity near the inlet is due to flow-related enhancement. Central peak is due to image acquisition during slow diastolic flow.

Figure 5

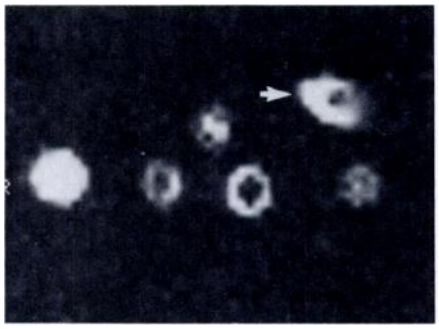

Oblique-flow phantom. There is signal loss upstream and increased signal on downstream end of vessel as it obliquely traverses the section (arrow).

were compared in all experiments to assess potential effects of partial magnetization at high velocity.

Steady flow was achieved using a large gravity feed tank, the flow rate being adjusted by varying the relative elevations of the influx and efflux lines. Entrance conditions were adjusted to allow full development of laminar flow within the afferent limb of the phantom at low velocities. Timed drainage into a graduated cylinder provided a measure of volumetric flow rate.

MR imaging was performed both clinically and on the flow phantom using a Diasonics 0.35-Tesla superconducting whole-body imager, which has been described previously (14). Spin echo (90°-180°-180°) sequences were used exclusively with repetition times (TR) of 0.5, 1.0, or 1.5 seconds and echo delay times (TE) of 28 and 56 msec. Images were acquired using the two-dimensional Fourier transform (2DFT) technique. Multisection acquisition provided 5, 10, or 15 sections during the period of time required to image a single section. A 128 × 128 acquisition matrix was used, corresponding to spatial resolution of 1.7 mm in the plane. Sections were 7 mm thick and spaced at 10-mm intervals (resulting in a 3-mm gap between sections). The flow phantom was positioned over a fat phantom in the center of a 30-cm head coil to simulate conditions of clinical imaging. The intensity recorded for the intraluminal signal was averaged over 12 to 16 pixels from a circular region of interest in the center of the tube. These pixels were chosen specifically to avoid boundary layer effects at the tube surface.

The intensities from the flowing and stationary water were measured for steady volumetric flow rates of 20 to 1,000 ml/min. First and second echo measurements were recorded from the first section encountered by the afferent and return limbs of the phantom. First and second echo intensities were compared at TR 0.5 sec to assess "even echo rephasing." In an attempt to analyze phase changes during slow flow through a magnetic field gradient, simulation using a DEC PDP11/45 computer was performed. Phase accumulation was calculated for groups of protons flowing at different velocities into a linear magnetic field gradient. Details of this computation have been reported previously (12).

First and second echo signals were compared over a wide range of flow velocities at TR 0.5 and TR 1.0 sec to evaluate "flow related enhancement." Diminishing intraluminal signal at higher velocity permitted evaluation of "high velocity signal loss." Oblique flow was investigated by positioning additional loops of tubing at 30° (afferent limb) and 60° (return limb) to the longitudinal axis of the magnet.

Pulsatile flow was investigated using a blood perfusion pump (Medical Engineering Consultants, Los Angeles, CA). To evaluate the effect of chance synchronization of the cardiac cycle and the MR repetition rate, the pulse rate of the perfusion pump was set to 40/min and the TR of the imager was set to 1.5 sec. This sequence produces 15 sections that are acquired sequentially every 100 msec. Intensities for the pulsatile flowing water and for the adjacent stationary water were measured for the 15 sections, several sections being imaged during systole (flow) and several during diastole (no flow).

RESULTS

Since the absolute intensity of the intraluminal signal is less important than the intensity relative to adjacent stationary tissue, the flow phantom data are plotted as a ratio (I/I_0) of flowing to stationary water. Not only did this negate the potential effects of radiofrequency (RF) nonuniformity in the coil, it also allowed us to neglect the complicating effects of differences in

the T1 and T2 relaxation times between the flowing and stationary substances.

"Flow-related enhancement" was evaluated by measuring the intensity of the intraluminal signal at different flow rates. Measurements were made in the first section encountered by the flowing water where the effect is expected to be greatest (7). The ratio of the intensities of the flowing to stationary water was plotted as a function of measured volumetric flow rate for TR values of 0.5 and 1.0 seconds (Fig. 2). At the shorter repetition time, flow-related enhancement was greater and occurred at higher velocity.

Progressive loss of signal was noted (Fig. 2) as the flow rate increased beyond that of maximal flow-related enhancement. This reflects "high velocity signal loss" initially and then onset of turbulence (15).

The first and second echoes in an echo train are plotted as a function of flow rate in Figure 3. These data are recorded in the first section encountered by the flowing water and thus include the effects of flow-related enhancement. The stronger signal coming from the second (56 msec) spin echo relative to the first (28 msec) demonstrates "even-echo rephasing."

A potential source of increased intraluminal signal during pulsatile flow is shown in Figure 4. Here the ratio of intensities of flowing to stationary water is plotted as a function of distance into the volume imaged during a 15-section acquisition. The perfusion pump pulse rate of 40/min and the TR of 1.5 sec were expected to synchronize the systolic or diastolic portions of the cardiac cycle to particular sections in the volume imaged. When the pulse rate and repetition time are matched in this manner, each section is effectively gated, *i.e.*, it is acquired only during a particular phase of the cardiac cycle. The central peak of increased intraluminal signal in Figure 4 represents sections imaged during the diastolic portion of the cycle, while the remainder were imaged during systole. The higher intensity in the sections near the entry surface represents flow-related enhancement.

An image from the oblique flow phantom is shown on Figure 5. Loss of signal is noted on the upstream side of the tubing and increased signal is present downstream. Recognition of this pattern permits determination of the direction of flow.

Figure 6

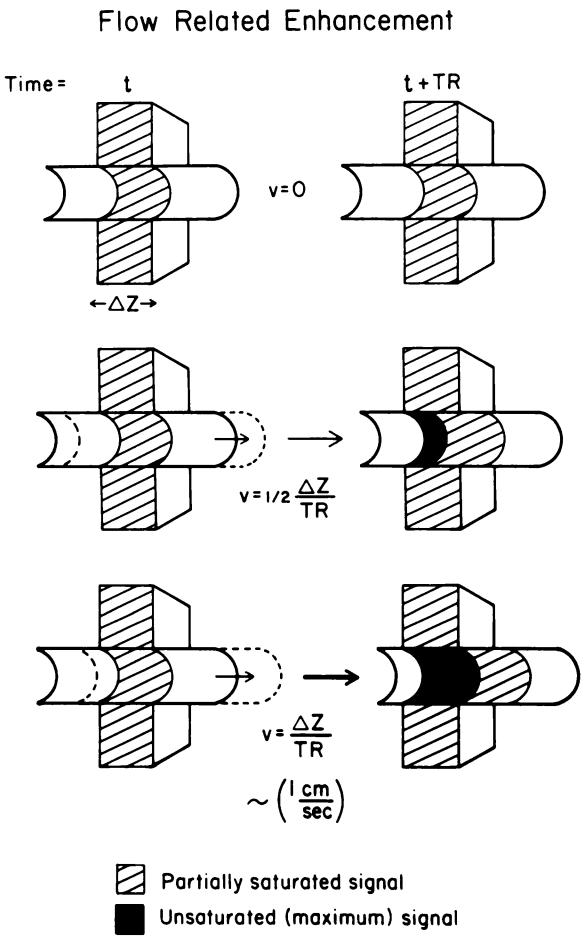

Flow-related enhancement. Under conditions of slow laminar flow, unsaturated protons enter section with full magnetization and emit stronger signal than protons in adjacent, partially saturated, stationary tissue. Maximum effect occurs when velocity = section thickness (Δz)/TR.

DISCUSSION

Water was used during these experiments rather than blood or a paramagnetic aqueous solution both for simplicity of experimental design and to exclude additional phenomena, such as the differences between the magnetic relaxation times of the blood and those of the adjacent stationary tissue, or the presence of "plasma skimming," which may occur during blood flow (13). Despite the longer T1 time of pure water (compared with blood), it is essentially fully magnetized by the time it reaches the center of the magnet where the flow phantom is positioned. Water in the afferent limb travels a distance of 1 meter within the magnet before reaching the phantom. Assuming a T1 relaxation time for water of 2.7 sec (16), 95% magnetization is achieved in 8 sec (17). Thus for velocities less than 100 cm per 8 sec (12.5 cm/sec), or volumetric flow rates less than 600 ml/minute, the water will be 95% magnetized. Water in the return loop travels an additional 2 meters through the magnet before returning to the phantom, thus it will be fully magnetized for velocities less than 25.0 cm/

Figure 7

Flow-related enhancement and high-velocity signal loss in a patient with carcinoma of the bladder. Increased signal in slow-flowing femoral veins (arrow) is due to unsaturated protons entering section. Absence of signal from the adjacent femoral arteries (arrowhead) reflects loss of signal due to turbulence and to protons leaving section prior to emission of spin echo.

Figure 8

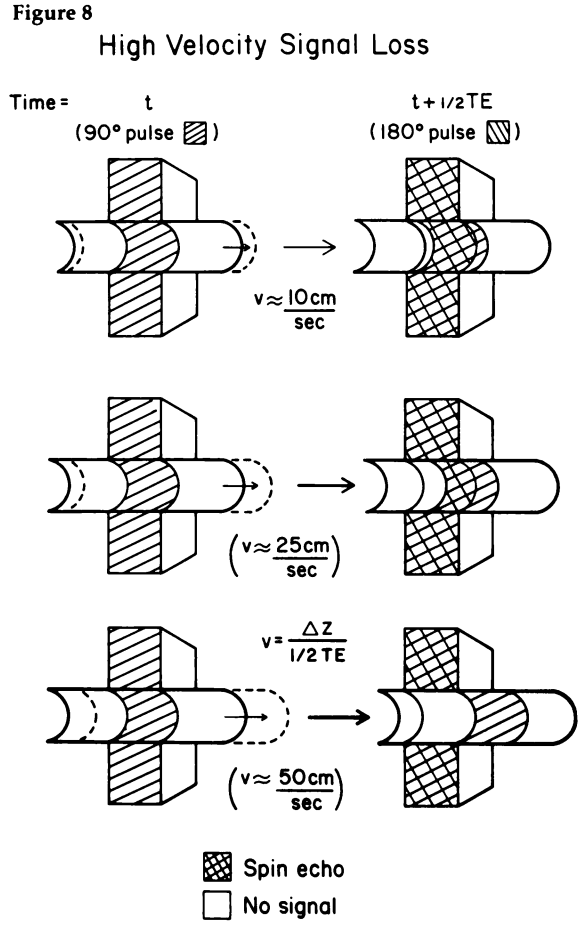

High-velocity signal loss. Protons must acquire both 90° pulse and 180° pulse to emit spin echo (crosshatch). Protons that acquire 90° pulse and then leave section prior to acquiring 180° pulse emit no signal. Protons flowing into the section following selective 90° pulse also emit no signal.

Figure 9

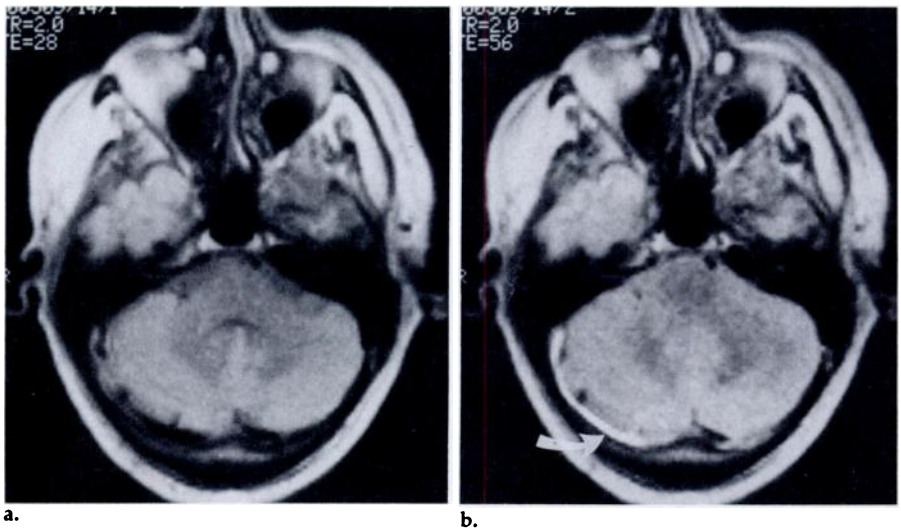

a. b.

Even-echo rephasing. Comparison of first 28-msec spin echo image (**a**) with second 56-msec spin echo image (**b**) demonstrates increased signal in the right transverse sinus (arrow). This is due to rephasing of isochromats in slow laminar flow.

sec and volumetric flow rates less than 1200 ml/min.

Flow-Related Enhancement

When slowly flowing blood enters the first section of a multisection volume, partially saturated blood remaining from the previous sequence is replaced by totally unsaturated blood (Fig. 6). The signal elicited from unsaturated blood is comparable with full magnetization (2–4) while the adjacent stationary tissue remains partially saturated to a degree depending on its own T1 relaxation time and the repetition time TR. The signal elicited from the flowing blood within the vessel comes from two populations of protons: a strong signal arising from the unsaturated, upstream protons and a weaker signal arising from the protons in the downstream portion of the voxel that were within the section at the time of the previous excitation. At the flow rate where all the blood in the voxel is replaced between averages, the signal is greatest. This occurs at velocity v:

$$v = dz/TR \qquad (1)$$

For a section thickness dz of 1 cm and a repetition time TR of 1 second, this corresponds to a velocity of 1 cm/sec.

The degree of "enhancement" of the flowing blood is really due to the limited longitudinal recovery of the adjacent stationary tissue in the time between repetitions. The effect is greater for stationary tissues with longer T1 relaxation times. Flow-related enhancement is also more pronounced at shorter repetition times, which allow less longitudinal recovery in the adjacent stationary tissue. This is supported by the experimental data shown in Figure 2. Equation 1 indicates that maximal flow-related enhancement occurs at higher velocities as the repetition time is decreased. This is also confirmed by the experimental data.

Flow-related enhancement effects are seen routinely during clinical MR imaging. Figure 7 demonstrates flow-related enhancement in the slow-flowing femoral veins while there is absence of signal from the adjacent femoral arteries. Loss of signal can result from two effects: high velocity and turbulence (15).

High Velocity Signal Loss

Loss of signal at high velocity is shown experimentally in Figures 2 and 3. This occurs when the protons exposed to the initial 90° pulse flow completely out of the section during the interpulse interval, prior to exposure to the 180° pulse (Fig. 8). Protons that flow into the section during the

interpulse interval have not received the 90° pulse and therefore will not emit a spin echo. Signal is lost from protons that flow a distance of one section thickness dz during the interpulse interval $\frac{1}{2}TE$, *i.e.*, at velocity v:

$$v = dz/\frac{1}{2}TE \qquad (2)$$

For a section thickness of 7 mm and an echo delay time of 28 msec, this corresponds to a velocity of 50 cm/sec. For the second echo at 56 msec, no signal is received from protons that do not remain within the section for a period of 42 msec, the time between the 90° pulse and the second 180° pulse. This corresponds to a velocity of 16.7 cm/sec. Total loss of signal is thus expected at lower velocities for second (and subsequent) echoes in a multiecho train than for the first echo. This is demonstrated experimentally in Figure 3.

Additional loss of signal is expected due to onset of turbulence (15). Turbulence can result either from the pulsatile, to-and-fro motion of the blood or from high velocity such that the Reynolds number exceeds 2100 (Reynolds number = tube diameter × velocity × density/viscosity) (18). Particularly rough, irregular surfaces and vascular branching can lead to turbulence at even lower velocities (19). When discussing turbulence, it is useful to consider a hypothetical, microscopic group of protons that travel as a group and all experience essentially the same magnetic field. Since they remain in phase, they have been called "isochromats" by Hahn (20). When the flow rate increases to the point where turbulence is present, random motion of isochromats causes additional loss of coherence. This random motion of the isochromats in turbulent flow is similar to the randomly fluctuating internal fields, which lead to T2 relaxation and loss of spin echo signal intensity. Loss of signal intensity with onset of turbulence is at variance with the discussion of Mills *et al.* (4) and is described further in Bradley *et al.* (15).

Even-Echo Rephasing

In Figure 9 the slow-flowing blood in the right transverse sinus has a significantly stronger signal on the 56-msec spin echo than on the initial 28-msec echo. Since the first echo is weak, this effect is not flow-related enhancement. This is seen frequently in large veins and dural sinuses and is associated with slow laminar flow (12). The stronger second echo is due to a rephasing phenomenon that occurs after each 360° of rotation following the initial 90° pulse, that is, for all even echoes in an echo train. Even-echo rephasing in slow flow has previously been combined with flow-related enhancement under the term "paradoxical enhancement" (3, 4). Appreciation of this phenomenon requires an understanding of the phasing and dephasing that occur during the spin echo sequence.

Figure 10 is a schematic diagram of the Carr Purcell Meiboom Gill spin echo sequence (21). Following the 90° pulse, isochromats begin to get out of phase due to magnetic field nonuniformities. Isochromats in a slightly stronger part of the field precess at a higher frequency and tend to get ahead of those in weaker parts of the magnetic field. This results in flaring of the magnetization vectors in the rotating reference frame shown in Figure 10. Following a 180° rotation about the y axis, dephased isochromats are flipped so that those that led now lag. Since they remain in a slightly stronger part of the magnetic field, however, they continue to precess at the higher frequency and eventually catch up to their more slowly precessing counterparts to generate a spin echo.

The same phenomenon can be

Figure 10

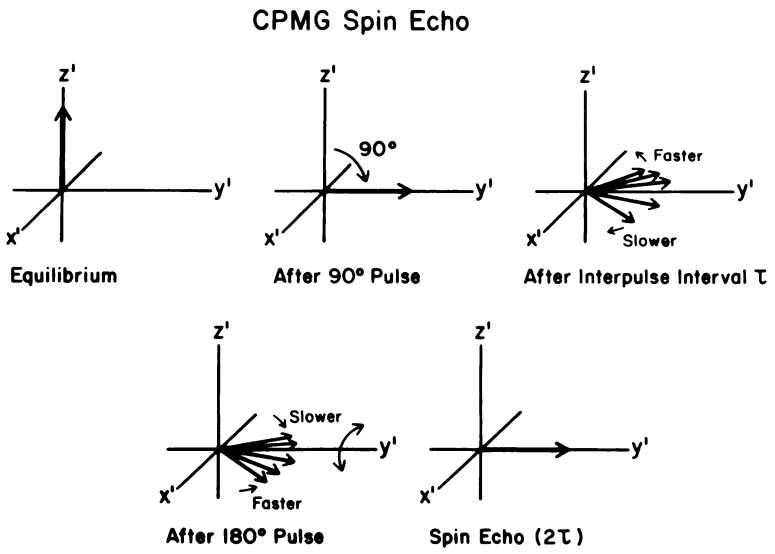

Carr Purcell Meiboom Gill (CPMG) spin echo. In rotating reference frame, magnetization (solid arrow) is rotated into x'–y' plane by 90° radiofrequency (RF) pulse. Dephasing causes flaring of the magnetization as some protons precess faster and some slower than average (due to relatively stronger and weaker local magnetic field). After interpulse interval τ 180° pulse is applied that causes rotation about y' axis and flared magnetization vectors begin to rephase. At 2τ rephasing is complete and coherent spin echo is emitted.

Figure 11

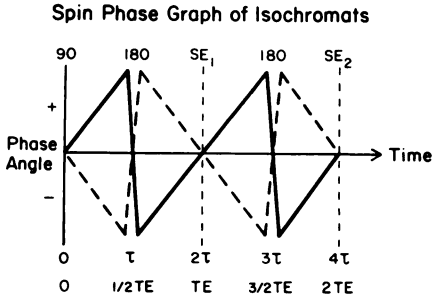

Spin phase graph. Phase is either lost or gained relative to average precessional frequency by protons in weaker and stronger parts of the magnetic field. Sign of phase is reversed by each 180° pulse (at τ and 3τ). Coherence is re-established at the time of each spin echo (SE_1 and SE_2).

Figure 12

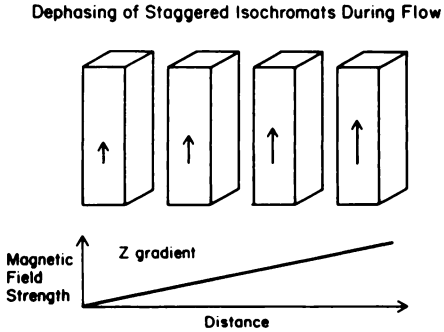

Dephasing of staggered isochromats during flow. Four isochromats are shown flowing into increasing (section-selecting) z gradient. Isochromats on leading edge of voxel are in stronger magnetic field (indicated by longer arrow) than isochromats on lagging edge. Isochromats on leading edge gain phase more rapidly than those behind.

Figure 13

Accelerated Phase Gain Due To Flow Into an Increasing Magnetic Field

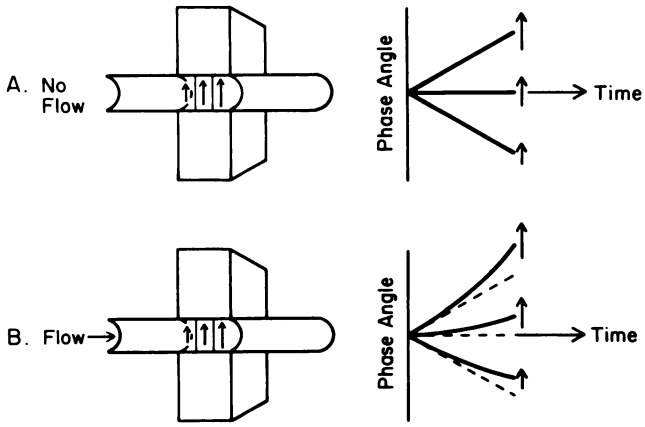

Accelerated phase gain due to flow into an increasing magnetic field. When a gradient is present without flow (**A**), rephasing occurs as it would in any other nonuniform magnetic field. When blood flows into an increasing magnetic field (**B**), phase is gained more rapidly than if the blood were stationary.

Figure 14

Blood Flow in a Magnetic Field Gradient

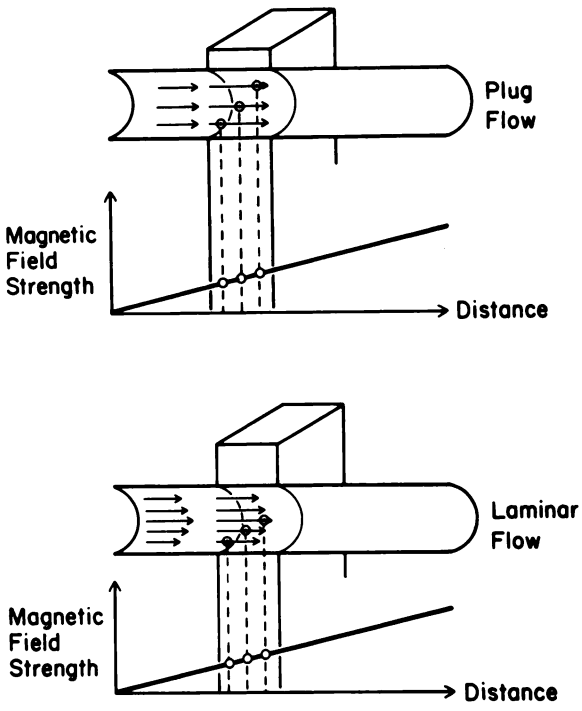

Blood flow in a magnetic field gradient. In plug flow all isochromats move at the same velocity. Phase gain is proportional to this velocity and to position in the voxel. Isochromats on the leading edge of the voxel gain phase more rapidly than those on the lagging edge. In laminar flow, isochromats in the center of the tube move at a higher velocity than those near the periphery. Protons on the leading edge of the voxel gain phase more rapidly not only due to position in the voxel but also because they flow at a higher velocity than those at the periphery.

demonstrated by the spin phase graph that was introduced by Singer (22). As shown in Figure 11, isochromats in a stronger part of the field gain phase until the 180° pulse when phase is reversed and they suddenly lose exactly the amount of phase they had just gained. They continue to gain or lose phase at the same rate and regain coherence with their more slowly precessing counterparts at the time of the spin echo. At this time, there is no difference in phase angle between different portions of the voxel. If the isochromats are allowed to dephase after the first spin echo, they can be rephased by a second 180° pulse, producing a second spin echo.

If blood flows into an increasing magnetic field gradient (Fig. 12), isochromats on the leading edge of the voxel start in a stronger part of the magnetic field and gain phase more rapidly than those on the lagging edge, in the weaker part of the magnetic field. If there were no flow in the vessel, isochromats in different portions of the magnetic field would dephase as they do in any other nonuniform magnetic field (Fig. 13A). When there is flow into an increasing magnetic field gradient the phase changes can no longer be represented by straight lines but are now quadratic curves, which gain phase somewhat more rapidly (Fig. 13B).

If all isochromats were to move at the same velocity (as in plug flow) they would each increase in phase at the same rate. When laminar flow is present, a parabolic profile exists so that the protons in the center of the stream move at a higher velocity than those at the periphery (Fig. 14). Protons in the center of the stream are also on the leading edge of the voxel and therefore are in a stronger field. These isochromats gain phase at an even greater rate than those on the lagging edge. At the time of the first spin echo, coherence is not totally regained, as there is a phase difference between isochromats on the leading and lagging edges of the voxel. Following an additional 180° of rotation for the second echo, that phase difference is corrected so that coherence is re-established (12).

Loss of intensity in the first echo can be considered analogous to partially reversible loss of coherence during a free induction decay (FID), which primarily reflects fixed field nonuniformities. In this sense, the temporary lack of coherence at the time of the first spin echo in laminar flow might be compared with loss of coherence in an FID that is regained at the time of the spin echo.

This effect is demonstrated on the

computer simulations in Figures 15 and 16 showing plug flow and laminar flow into an increasing magnetic field gradient (12). The two simulations shown are for equal volumetric flow rates and indicate a much greater phase difference for laminar flow than for plug flow at the time of the first spin echo. Coherence is totally re-established following 360° rotation at the time of the second spin echo for both flow situations. The amount of phase difference at the time of the first echo in laminar flow increases as the flow rate increases and the parabolic profile steepens, increasing the range of velocities present. Thus the first echo becomes less intense relative to the rephased second echo as the velocity increases. This is shown in Figure 3. At velocities greater than that of the maximum rephasing effect, the difference in intensities between the two echoes decreases due to high velocity signal loss. Eventually the intensities of the two echoes become equal as the enhancing effect of rephasing is countered by the increased signal loss due to high velocity. As the velocity continues to increase, the second echo becomes progressively weaker than the first and eventually all signal is lost.

Figure 15

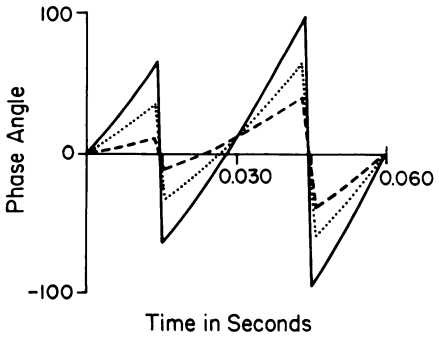

Computer simulation of plug flow. Phase angle of isochromats in stronger half of field is plotted as a function of time (spin echoes occur at 0.030 and 0.060 sec). Positive phase angle at time of first spin echo indicates lack of total rephasing although spread of phase angles at 0.030 sec is minimal. Complete rephasing occurs on the second spin echo at 0.060 sec.

Figure 16

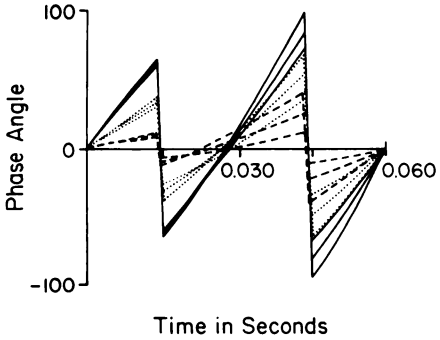

Computer simulation of laminar flow. Phase angle of isochromats at different positions in voxel field are plotted as a function of time with spin echoes occurring at 0.030 and 0.060 sec. Three groups of three curves each are shown. Within each group the isochromats that gain most rapidly are in the center of the tube where flow velocity is greatest. Group with solid lines is on leading edge of voxel in stronger part of gradient field. Group with dashed line is on lagging edge of voxel in weaker portion of gradient field. Spread of phase angles at 0.030 sec is seen to be significantly greater than during plug flow. This lack of complete rephasing decreases the intensity of the first spin echo. Complete rephasing is present at the time of the second spin echo at 0.060 sec.

Diastolic Pseudogating

When the cardiac cycle and the repetition time are synchronized, each section in a multisection acquisition is acquired at the same time in the cardiac cycle. When MR acquisition is electronically gated to the EKG, the intraluminal signal is expected to increase when flow slows during diastole. This is demonstrated on EKG-gated MR images in Figure 17.

In certain circumstances, although MR acquisition is not gated to the EKG, chance synchronization of the cardiac cycle and the MR acquisition sequence may result. When the interval between heart beats and the repetition time TR (or an integral multiple thereof) are the same, this will occur, *e.g.*, for a pulse of 60 and a TR of 1.0 sec. We call this "pseudogating." When certain sections are imaged during diastole, increased intraluminal signal will result, as shown in Figure 4. To exclude diastolic pseudogating as a cause of intraluminal signal, gated imaging during cardiac systole may be necessary.

Oblique Flow

The appearance of blood flowing oblique to the imaging plane can be a source of both information and confusion. As shown in Figure 5, signal loss occurs on the upstream side of the section while signal is increased on the downstream side. If the section-defining gradient is off between the selec-

Figure 17

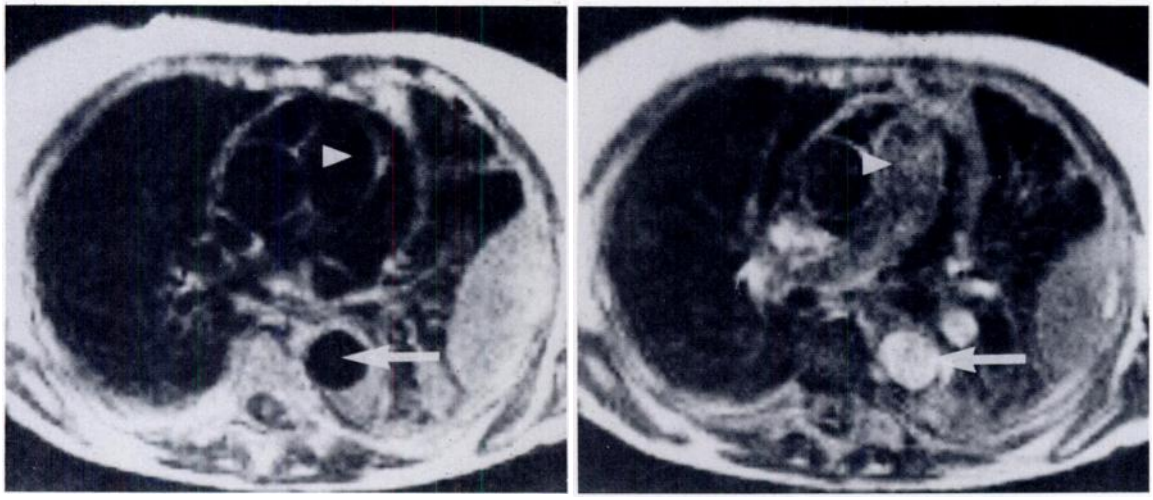

a. b.

Systolic and diastolic gated MR images.

a. Lack of signal in ascending and descending aorta (arrow) and pulmonary outflow (arrowhead) tract during rapid, turbulent flow in systole. (Note also left pleural effusion.)

b. Increased signal in aorta (arrow) and pulmonary artery (arrowhead) due to slowed flow present during mechanical diastole (section 1 cm cephalad to **a**).

Figures 18 and 19

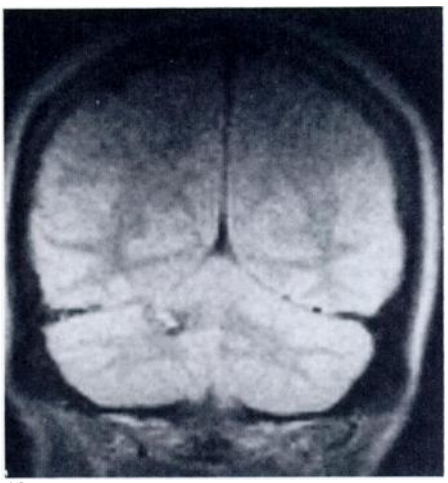

18.

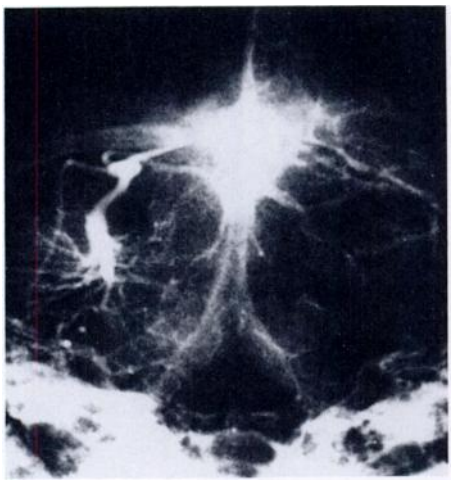

19.

18. Cerebellar venous angioma (TR = 2.0 sec, TE = 28 msec). Coronal section. Decreased signal seen inferiorly with increased signal superiorly. When flow is oblique to the imaging plane, the signal is increased on the downstream side of the section.
19. Angiogram showing flow in venous angioma from medial inferior to lateral superior.

tive 180° pulse and acquisition of the spin echo, the downstream signal actually includes protons that have flowed out of the section after the 180° pulse, increasing the signal. When flow is perpendicular to the imaging plane these effects are averaged together in the total intraluminal signal. This may explain the broad peaks noted in Figure 2.

When flow is oblique to the imaging plane, the direction of blood flow can occasionally be predicted. In Figure 18 flow would be predicted from medial and inferior to lateral and superior in the cerebellar venous angioma. This is confirmed by the angiogram in Figure 19.

Oblique flow can also be a potential source of confusion. The combined appearance of increased signal and absent signal within the lumen may be mistaken for intraluminal thrombus or tumor.

SUMMARY

Using a flow phantom, computer simulation, and clinical examples, the variable appearance of flowing blood observed during clinical MR imaging has been evaluated. The intraluminal signal is increased in several circumstances. When unsaturated protons first enter the imaging volume they elicit a strong signal relative to the partially saturated surrounding tissue (flow-related enhancement). The second (or any even) echo is increased relative to the first (or odd echoes) due to rephasing of isochromats during slow laminar flow. When the cardiac cycle and the MR pulsing sequence happen to become synchronized, increased signal is found on sections imaged during diastole (diastolic pseudogating). Loss of intraluminal signal can be due to high velocity or onset of turbulence. When flow is oblique to the imaging plane, decreased upstream and increased downstream signal allows one to predict direction of flow.

Acknowledgment: We wish to thank Kaye Finley for manuscript preparation, Keith E. Kortman, M.D., for manuscript review, and Leslee Watson, Terry Andrues, and Jay Mericle for technical assistance.

NMR Imaging Laboratory
Huntington Medical Research Institutes
10 Pico Street
Pasadena, CA 91105

References

1. Hawkes RC, Holland GN, Moore WS, Worthington BS. Nuclear magnetic resonance (NMR) tomography of the brain: a preliminary clinical assessment with demonstration of pathology. J Comput Assist Tomogr 1980; 4:577–586.
2. Crooks L, Sheldon P, Kaufman L, Rowan W, Millter T. Quantification of obstructions in vessels by nuclear magnetic resonance. IEEE Trans Nucl Sci 1982; NS-29:1181.
3. Crooks LE, Mills CM, Davis PL, et al. Visualization of cerebral and vascular abnormalities by NMR imaging. The effects of imaging parameters on contrast. Radiology 1982; 144:843–852.
4. Mills CM, Brant-Zawadzki M, Crooks LE, et al. Nuclear magnetic resonance: principles of blood flow imaging. AJNR 1983; 4: 1161–1166.
5. Young IR, Burl M, Clarke GJ, et al. Magnetic resonance properties of hydrogen: imaging the posterior fossa. AJR 1981; 137:895–901.
6. Gore JC. The meaning and significance of relaxation in NMR imaging. In: Witcofski RL, Karstaedt N, Partain CL, eds. Proceedings of the NMR Symposium, Oct. 1–3, 1981. Winston-Salem, NC: Bowman-Gray School of Medicine Press, 1981.
7. Kaufman L, Crooks L, Sheldon P, Hricak H, Herfkens R, Bank W. The potential impact of nuclear magnetic resonance imaging on cardiovascular diagnosis. Circulation 1983; 67:251–257.
8. Moran P. A flow velocity zeugmatographic interlace for NMR imaging in humans. Magn Reson Imaging 1982; 1:197–203.
9. Singer JR, Crooks LE. Nuclear magnetic resonance blood flow measurements in the human brain. Science 1983; 221:654–656.
10. Axel L. Approaches to nuclear magnetic resonance (NMR) imaging of blood flow. Proc SPIE 1983; 347:336–341.
11. Wehrli FW, MacFall JR, Axel L, Shutts D, Glover GH, Herfkens RJ. Approaches to in-plane and out-of-plane flow imaging. Noninvasive Medical Imaging 1984; 1: 127–136.
12. Waluch V, Bradley WG. NMR even echo rephasing in slow laminar flow. J Comput Assist Tomogr 1984; 8:594–598.
13. George CR, Jacobs G, MacIntyre WJ, et al. Magnetic resonance signal intensity patterns obtained from continuous and pulsatile flow models. Radiology 1984; 151: 421–428.
14. Crooks L, Arakawa M, Hoenninger J, et al. Nuclear magnetic resonance whole-body imager operating at 3.5 KGauss. Radiology 1982; 143:169–174.
15. Bradley WG, Waluch V, Fernandez E, Spalter C. Magnetic resonance appearance of rapidly flowing blood. AJR, in press.
16. Fullerton GD, Cameron IL, Ord VA. Frequency dependence of magnetic resonance spin lattice relaxation of protons in biological materials. Radiology 1984; 151:135–138.
17. Bradley WG, Crooks LE, Newton TH. Physical principles of NMR. In: Newton TH, Potts DG, eds. Advanced imaging techniques. Vol II. San Francisco: Clavadel Press, 1983:Chapter 3.
18. McDonald DA. Blood flow in arteries. Baltimore: Williams and Wilkins Company, 1960.
19. Bird RB, Stewart WE, Lightfoot EN. Transport phenomena. New York: John Wiley and Sons, 1960.
20. Hahn EL. Spin echoes. Phys Rev 1950; 80:580–594.
21. Farrar TC, Becker ED. Pulse and Fourier transform NMR: Introduction to theory and method. New York and London:Academic Press, 1971.
22. Singer JR. NMR diffusion and flow measurements and an introduction to spin phase graphing. Phys E Sci Instrum 1978; 11: 281–291.